

Direct Analysis of Sugar Alcohol Borate Complexes in Plant Extracts by Matrix-Assisted Laser Desorption/Ionization Fourier Transform Mass Spectrometry

Sharron G. Penn,[†] Hening Hu,[‡] Patrick H. Brown,[‡] and Carlito B. Lebrilla^{*,†}

Departments of Chemistry and Pomology, University of California, Davis, California 95616

Matrix-assisted laser desorption/ionization Fourier transform mass spectrometry (MALDI/FTMS), operating in the negative ion mode, is used to directly observe sugar alcohol borate complexes in a number of plant fractions. The method involves virtually no sample workup and, in the case of celery phloem sap, requires only 40 nL of sap to observe the borate complex. The isolation and characterization of such soluble borate complexes is important in understanding the distribution of boron in plants. The results show that the complexes are composed of two mannitol or sorbitol ligands (L) complexed to a single borate center (B). In some cases, the boron is complexed to non-alditol monosaccharides. Sustained off-resonance collision irradiation dissociation of the BL₂⁻ complex, where L is a mannitol, gives fragments that confirm the proposed structure. Complexes of larger oligosaccharides have also been successfully observed using MALDI/FTMS. Semiempirical molecular orbital calculations (AM1) of the mannitol BL₂⁻ complex show that the most favorable configuration is with carbons 3 and 4 of both mannitol residues complexed to the borate. This allows maximum interaction of the remaining hydroxyls with the borate center.

It has been known for nearly 50 years that borate will complex with diols in solution.¹ While there is much work in the literature on the investigation of borate polyol complexes by nuclear magnetic resonance (NMR) spectroscopy,² particularly with carbohydrates,^{3–6} there have been only been a few reports on the use of mass spectrometry to investigate borate complexes. Rose and co-workers⁷ used both fast atom bombardment (FAB) and negative ion electrospray (ESI) to investigate a number of boron acids, showing that both techniques give excellent results. They originally postulated that ESI might lead to hydrolysis of the borates, but using water/acetonitrile as the solvent gave mostly

the intact anion if samples were analyzed within 1 h of preparation. Lipták and co-workers⁸ used thermospray MS to study complex formation between polyols, carbohydrates, and borate in the positive ion mode. They found that they could determine isomeric differences in small systems, but for larger carbohydrates this was more difficult, as the spectra became more complicated.

Boron is one of the essential elements in plant growth.⁹ Its primary function, however, is still not fully understood, but the uptake, transport, and function of boron appears to be dependent on the formation of boron complexes.^{10,11} The characterization of the soluble borate complexes found in plants helps to understand the role of boron, an important question in the agricultural sciences.^{10,11} Until now, there has been little direct observation of these complexes in plant tissues. The boron content of plant tissues has been monitored using inductively coupled plasma mass spectrometry (ICPMS)¹² high-performance liquid chromatography (HPLC), and gas chromatography/mass spectrometry (GC/MS)¹³ has been used to identify the saccharides present.

Recently, Kobayashi et al.¹⁴ isolated a boron–polysaccharide complex from radish root cell walls. Using MALDI/TOFMS, with a N₂ laser at 337 nm and 2,5-dihydroxybenzoic acid as matrix, they found that the molecular mass of the complex before acid hydrolysis was 9894 Da, and after acid hydrolysis it was found to be 4927 Da (masses reported by Kobayashi et al.¹⁴). From these data the workers concluded that the complex was made up of two identical halves, bound together by boron. Using ¹¹B NMR, they also showed that the boron was present as a tetravalent 1:2 borate–diol complex, and gravimetric data showed that the borate:sugar ratio was 1:2.

In this paper, we use MALDI/FTMS to directly observe borate complexes in plant extracts. MALDI/FTMS is ideally suited to the analysis of plant extracts, since no sample pretreatment or purification is required, only very small sample volumes are needed, and the high mass accuracy and resolution can show elemental composition¹⁵ and isotope patterns clearly, particularly

[†] Department of Chemistry.

[‡] Department of Pomology.

- (1) Boeseken, J. *Adv. Carbohydr. Chem.* **1949**, *4*, 189.
- (2) Reed, D. *Chem. Soc. Rev.* **1993**, *22*, 109–116.
- (3) Takeda, T.; Oi, T.; Yoshimura, K.; Miyazaki, Y.; Sawada, S.; Waki, H. *J. Chem. Soc., Faraday Trans.* **1996**, *92*, 651–656.
- (4) Vandenberg, R.; Peters, J. A.; Bekkum, H. v. *Carbohydr. Res.* **1994**, *253*, 1–12.
- (5) VanHaveren, J.; Vandenburg, M. H. B.; Peters, J. A.; Batelaan, J. G. *J. Chem. Soc., Perkin Trans. 2* **1991**, *3*, 321–327.
- (6) Chapelle, S.; Verchere, J. F. *Carbohydr. Res.* **1989**, *191*, 63–70.
- (7) Rose, M. E.; Wycherlet, D.; Preece, S. W. *Org. Mass Spectrom.* **1992**, *27*, 876.

- (8) Lipták, M.; Dinya, Z.; Herczegh, P.; Jeko, J. *Org. Mass Spectrom.* **1993**, *28*, 780–784.
- (9) Loomis, W. D.; Durst, R. W. *Biofactors* **1992**, *3*, 229–239.
- (10) Brown, P. H.; Hu, H. N. *Physiol. Plant.* **1994**, *91*, 435–441.
- (11) Hu, H. I.; Brown, P. H. *Plant Physiol.* **1994**, *105*, 681–689.
- (12) Brown, P. H.; Picchioni, G.; Jenkin, M.; Mu, H. N. *Commun. Soil Sci. Plant. Anal.* **1992**, *23*, 2781–2807.
- (13) Albersheim, P.; Neivins, D. J.; English, P. D.; Karr, A. *Carbohydr. Res.* **1967**, *5*, 340–345.
- (14) Kobayashi, M.; Matoi, T.; Azuma, J. *Plant Physiol.* **1996**, *110*, 1017–1020.
- (15) Fannin, S. T.; Wu, J.; Molinski, T.; Lebrilla, C. B. *Anal. Chem.* **1995**, *67*, 3788–3792.

at the low masses expected in these samples. The use of theoretical calculations in an analytical problem can help us gain a better understanding of the possible structure of the complexes. We use semiempirical molecular orbital calculations to predict the lowest energy conformers of the complexes and connectivity. Since the borate complexes are in equilibrium, it is highly probable that they are under thermodynamic control, and hence molecular orbital calculations may provide a true representation of the species studied by MALDI.

EXPERIMENTAL SECTION

Sorbitol was obtained from Fisher (Fair Lawn, NJ), mannitol was obtained from Sigma (St. Louis, MO), and 2,5-dihydroxybenzoic acid (DHB) and 3-aminoquinoline (3-AQ) were obtained from Aldrich. All were used without further purification.

Plant extracts (phloem sap, juice, and extracellular nectar) were obtained as described previously.¹⁶ Briefly, leaves from 6-month-old celery (*Apium graveoleus*) plants were submerged in 50 mM boric acid solution, containing 0.05% (v/v) L-77 surfactant. Phloem sap was collected the following day by cutting the stems and collecting sap using a fine-tip glass microcapillary 200 μm in diameter. The capillary was placed directly in contact with the vascular tissue, and the exudate was collected by capillary action. Each cut surface yielded between 0.05 and 0.2 μL , and the procedure was repeated until 2–3 μL of sap was collected. The sap was kept in plastic tubes and maintained in an ice bath during collection. The sap was diluted 50-fold with Nanopure water, and 2 μL was used for analysis by MALDI/FTMS. The celery juice was collected by using the same kind of vascular tissue as for sap collection and squeezing until liquid was extruded. Sample pretreatment was slightly more complicated, due to the greater number of components that may be in the celery juice as compared to celery sap. The liquid was heated for 1 min in boiling water to denature any proteins and remaining chlorophyll. It was then filtered and diluted 8.3-fold. About 2 μL was used for analysis by MALDI/FTMS. Extrafloral nectar was collected from recently fully mature peach leaves. The nectar was diluted by 100-fold with Nanopure water, and about 2 μL was used for analysis by MALDI/FTMS.

The mass spectra were obtained using an external source Fourier transform mass spectrometer (HiResMALDI, IonSpec Corp., Irvine, CA) equipped with a 4.7 T magnet and a nitrogen laser at 337 nm. All spectra were obtained using 3-AQ as the matrix unless otherwise stated. The 3-AQ was used at a concentration of 0.4 M, dissolved in ethanol. Sample preparation involved depositing 2 μL of sample on the probe tip, followed by 1 μL of 3-AQ. The mixture was then dried in a cold air stream until crystals started to form. For method development experiments, sorbitol and mannitol samples were made up at the desired concentration in methanol.

Molecular orbital calculations were carried out using the SPARTAN program (Wavefunction Inc., Irvine, CA) on a Silicon Graphics workstation. Semiempirical calculations were run using the Austin method 1 (AM1) routine. At least eight minimizations were carried out on each structure, first carrying out a conformer search and then minimizing the most energetically favorable structures, first by molecular mechanics (SYBYL) and then by semiempirical methods (AM1).

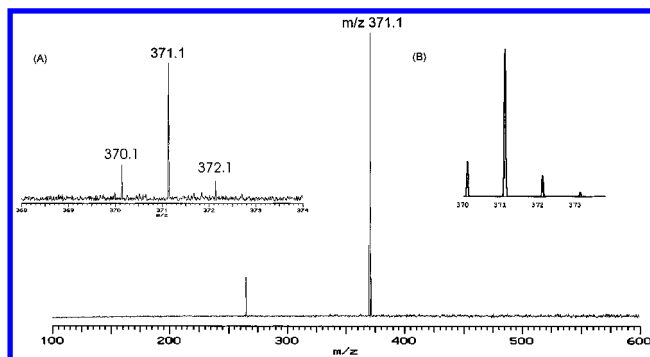


Figure 1. Negative mode MALDI/FTMS spectrum of 10 mM mannitol with 1 mM boric acid sample. Inset A shows expanded region of mass spectrum detailing the isotopic distribution. For other experimental details, see text. Inset B shows the computer-predicted isotopic distribution of BL_2^- , where L is mannitol or sorbitol.

RESULTS

MALDI/FTMS of Mannitol and Sorbitol Borate Complexes: Method Development. The choice of matrix appears to be key to the observation of sugar alcohol borate complexes. The most common matrix used for MALDI is DHB.¹⁷ However, when trying to observe negative ions in MALDI/FTMS using DHB as the matrix, a peak at m/z 153 was seen, corresponding to the deprotonated matrix ion. If borate was present with the matrix, the DHB effectively complexed with the borate in preference to the borate complexing with the sugar, and a prominent peak at m/z 315 was observed, corresponding to two doubly deprotonated DHB molecules bound together through boron produced by equilibrium during crystallization. For this reason, a matrix containing no oxygen atoms was chosen to eliminate the complexing of the matrix to the borate. 3-AQ satisfied this criterion. It is interesting to note that Kobayashi et al.¹⁴ used DHB for the analysis of the polysaccharide–boron complex from radish root. They were, however, analyzing the complex in the positive ion mode and thus would not observe the m/z 315 species discussed above.

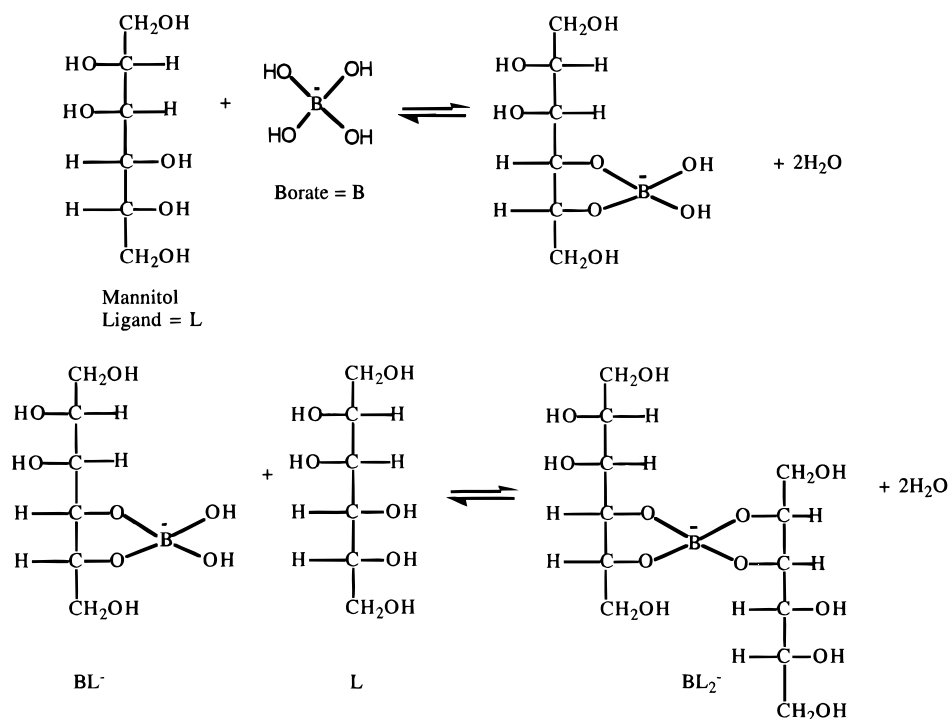
Previous work has shown that sorbitol and mannitol, isomers of open-chain monosaccharide alcohols, are found in plants and thus may be complexed to borate.^{10,11} Method development was therefore carried out on standard solutions containing mannitol and sorbitol with boric acid. Figure 1 shows the negative ion mode mass spectrum of 10 mM mannitol mixed with 1 mM boric acid and titrated to pH 7 with KOH. It is estimated that these are the concentrations of sugar alcohol and borate naturally occurring in the sap of species such as celery. The dominant peak is at m/z 371.1, corresponding to a complex of two sorbitols with borate, BL_2^- . This agrees with NMR studies that predict this form of borate–mannitol complex under these concentrations and pH.¹⁸ The equilibrium between the mannitol and borate resulting in the BL_2^- complex is shown in Scheme 1. In Scheme 1, the borate is attached to carbons 2 and 3. This scheme in no way indicates that carbon 2 and 3 are preferentially complexed but is drawn this way for clarity. Mass spectra of 10 mM sorbitol with 1 mM boric acid gave identical peaks. Since mannitol and sorbitol are isomers, we are unable to differentiate between them mass spectrometrically.

(16) Hu, H.; Penn, S. G.; Lebrilla, C. B.; Brown, P. H. *Plant. Physiol.* **1997**, *113*, 649–655.

(17) Strupat, K.; Karas, M.; Hillenkamp, F. *Int. J. Mass Spectrom. Ion Processes* **1991**, *111*, 89–102.

(18) Makkee, M.; Kieboom, A. P. G.; Bekkum, H. v. *Recl. Trav. Chim. Pays-Bas* **1985**, *104*, 230–235.

Scheme 1



Inset A of Figure 1 shows an enlarged area of the BL_2^- peak. Naturally occurring boron is present as two isotopes, 19.83% being ^{10}B and 80.17% being ^{11}B . This, coupled with the naturally occurring carbon isotope distribution, leads to the distinctive isotope pattern which is clearly seen. Inset B of Figure 1 shows the predicted distribution of the overlapping boron and carbon isotope patterns, and it can be seen that this agrees very well with the experimental distribution. At high concentrations, a complex of the form $B_2L_2H^-$ was observed (not shown). It was initially hoped that the formation of this diborate species may be a way to distinguish between the isomers mannitol and sorbitol. However, both sugar alcohols were capable of forming $B_2L_2H^-$.

Makkee et al.¹⁸ carried out a series of pH-dependent studies of mannitol–boric acid mixtures using ^{11}B NMR. For 1:1 ratios of mannitol to boric acid, they found that the concentration of BL^- increased with increasing pH, while the free borate anion decreased with increasing pH. The amount of BL_2^- increased slightly up to pH 8, and then fell again up to pH 12. However, using ^{11}B NMR, Makkee and co-workers¹⁸ were unable to differentiate between the species BL^- , B_2L^- , and B_3L^- . In MALDI, only the BL_2^- (m/z 371.1 for ^{11}B) species was observed at 1:1 concentrations at pH 7, along with a small amount of $B_2L_2H^-$ species (m/z 379.1 for ^{11}B); therefore, pH was varied in an attempt to observe the other species. The solutions were titrated to different pHs using concentrated KOH. Generally, as pH was increased, the signal:noise ratio of the spectra became worse, and it became increasingly difficult to find a position on the probe surface that gave signal (a “sweet spot”). At pH 9, only the BL_2^- complex was observed; however, at pH 11, no mannitol borate complex was observed.

While rigorous limits of detection were not pursued, it was still possible to observe BL_2^- borate complexes at concentrations of 1 mM sorbitol and 0.05 mM boric acid, the lowest concentrations analyzed. The largest sugar alcohol:boron ratio observed

was with 10 mM sorbitol and 0.1 mM boric acid, again the largest ratio analyzed.

Mannitol and sorbitol are open-chain alcohols, but it was also possible to form complexes of pyranose (six-membered ring) sugars, such as glucose. A spectrum of 10 mM fructose and 1 mM boric acid led to observation of the BL_2^- complex, resulting in peaks at m/z 366.1 ($^{10}BL_2^-$) and 367.1 ($^{11}BL_2^-$) (results not shown).

MALDI/FTMS of Plant Extracts. Figure 2 shows the mass spectrum of celery phloem sap. The celery plant had received boron application to the leaf to monitor phloem boron mobility in the plant. It is important to stress that minimal sample workup was required to obtain this spectrum. As stated in the Experimental Section, sap collected directly from the plant was diluted by a factor of 50 in Nanopure water, and 2 μ L of it was deposited directly on the MALDI probe tip. The sample required no filtering, extraction, or other purification techniques. In Figure 2, peaks are clearly observed corresponding to sorbitol and/or mannitol borate complexes at m/z 370.1, 371.1 and 372.1. In previous work¹⁶ using HPLC and GC/MS, the occurrence of mannitol in the phloem of celery was verified; therefore, it is highly likely that these peaks are due to mannitol borate complexes. It is also known that mannitol is the primary photosynthetic product in celery.¹⁹ From HPLC,¹⁶ it was estimated that the concentration of mannitol in the sap was 150–300 mM, while the boron was at a concentration of 1–1.5 mM one day after leaf application of boron, as determined by ICPMS. Therefore, from the NMR work by Makkee et al.,¹⁸ we once again expect to see the BL_2^- complex. The peak at m/z 369.1 is interesting since it corresponds to a complex of borate with a single mannitol and a single pyranose sugar (such a fructose or glucose), in the BL_2^- form. As previously mentioned, we have been successful in observing BL_2^-

(19) Davis, J. M.; Fellman, J. K.; Loescher, W. H. *Plant. Physiol.* **1988**, *86*, 129–133.

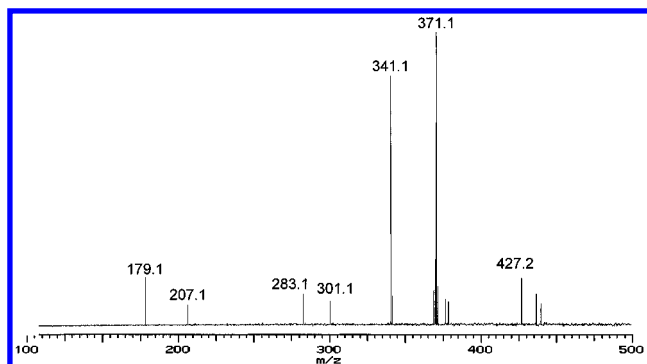


Figure 2. Negative mode MALDI/FTMS of phloem sap obtained from celery. For other experimental details, see text.

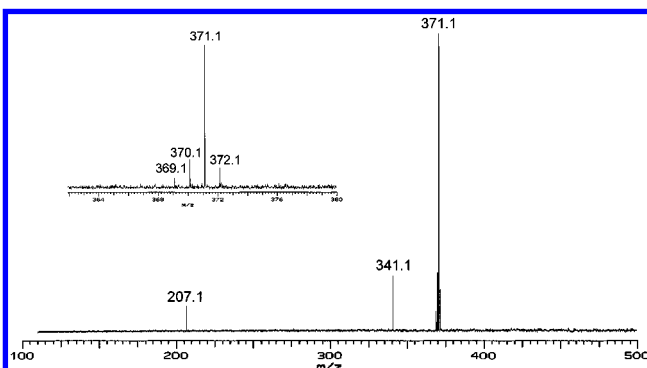


Figure 3. Negative mode MALDI/FTMS of phloem juice obtained from celery. For other experimental details, see text.

complexes of pyranose sugars in method development experiments (results not shown), but we are unable to assign which pyranose (fructose or glucose) is present in the peak at m/z 369.1. Since the sample had not been purified in any way, it is not possible to assign all the peaks in Figure 2, which may arise from other carbohydrates or peptides/amino acids found in the phloem sap. In experiments carried out over wider mass ranges (not shown), peaks are observed at higher masses. However, in Figure 2, the region m/z 365–375 contains the only peaks in the mass spectrum which show the distinctive boron isotope pattern. We believe m/z 179.1 is the $[M - H]^-$ ion of a pyranose sugar such as fructose, m/z 341.1 is the $[M - H]^-$ ion of a disaccharide (possibly sucrose, which together with mannitol are the two major carbohydrates in celery phloem¹⁹), and m/z 207.1 is a fragment of the mannitol BL_2^- peak. The peak at m/z 283.1 is due to a dimer of the matrix 3-AQ, identified from running a blank sample.

Figure 3 shows the mass spectrum of celery juice from the same plant. For this sample 10 μ L was deposited on the probe tip with 1 μ L of matrix. The spectrum in Figure 3 appears to be “cleaner” than in Figure 2, but it was more difficult to find a position on the probe tip that gave a good signal. Again, we observe peaks corresponding to mannitol and pyranose BL_2^- complexes at m/z 369.1, 370.1, and 371.1. The inset shows this region more clearly. We also observe a peak corresponding to deprotonated disaccharides at m/z 341.1, and a fragment of the complex at m/z 207.1.

Figure 4 shows the mass spectrum of extrafloral peach nectar from the species *Prunus*. It is technically easier to obtain this nectar than to obtain phloem sap from peach seedlings, and since the nectar is mainly supplied from the phloem, it should still be informative as to the composition of boron complexes in peach seedling phloem. In Figure 4, 1 μ L was deposited on the probe

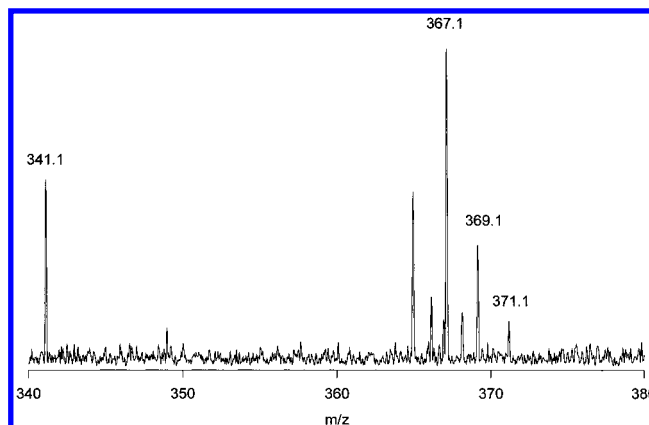


Figure 4. Negative mode MALDI/FTMS of extracellular nectar obtained from peach seedlings. For other experimental details, see text.

tip. The resulting spectrum is very complex, and many of the peaks are not assignable, since the sample may contain other sugars as well as amino acids and peptides. However, the region m/z 340–380 shows the BL_2^- complex very clearly. The dominant peak in this area appears to be at m/z 367.1. This corresponds to a pyranose (such as fructose) borate BL_2^- complex. Some sugar alcohol complex is observed at m/z 371.1. Loescher has shown that sorbitol is the primary photosynthetic product in *Prunus*,²⁰ therefore, we expect BL_2^- (m/z 371.1) to be a sorbitol borate complex. Once again, the relative concentrations of boron and sugar are such that we observe BL_2^- stoichiometry.

Collision-Induced Dissociation of the Mannitol Borate BL_2^- Complex. To gain further structural information on the mannitol borate complex (BL_2^-), collision-induced dissociation (CID) was carried out. On-resonance CID has previously been shown to give abundant structural information on oligosaccharides,²¹ but CID of this small complex resulted in the loss of signal before any fragments were observed. Presumably, the ion was excited to a radius larger than the ICR cell dimensions, and the ions were thus lost before any fragments were detected.

To overcome this problem, sustained off-resonance irradiation (SORI) CID was carried out. In this experiment, the m/z 371.1 ion was excited 500 Hz below the cyclotron frequency, corresponding to an m/z of 372.1, for a period of 1000 ms at 1.165 V. Under these conditions, the m/z 371.1 ion undergoes 500 oscillations, during which it can collide with the argon that is being pulsed into the chamber at a pressure of 9×10^{-6} Torr. Using standard equations,²² this results in the m/z 371.1 ion gaining an average translational energy of 9.6 eV, and a center of mass frame energy (E_{cm}) of 0.9 eV. However, because of the complicated isotopic pattern due to the boron under these experimental conditions, SORI CID was also inadvertently being carried out on the m/z 370.1 ion. In addition, on-resonance excitation of the m/z 372.1 ion was also occurring, which would result in the loss of ions as previously mentioned. Since it was not possible to completely isolate the ion at m/z 371.1, some ions at m/z 370.1 and 372.1 still remained in the cell. Therefore, we expected that the isotopic pattern of the resulting fragments would have “incorrect” proportions.

(20) Loescher, W. H. *Plant. Physiol.* **1987**, *70*, 230–235.

(21) Penn, S. G.; Cancilla, M. T.; Lebrilla, C. B. *Anal. Chem.* **1996**, *68*, 2331–2339.

(22) Marzluff, E. M.; Campbell, S.; Rodgers, M. T.; Beauchamp, J. L. *J. Am. Chem. Soc.* **1994**, *116*, 7787–7796.

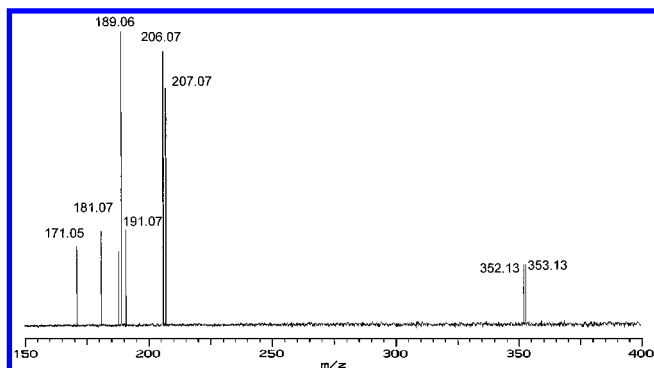


Figure 5. SORI CID spectrum of the BL_2^- mannitol complex. The m/z 371.1 ion was excited 500 Hz below the cyclotron frequency for a period of 1000 ms at 1.165 V. The ion underwent 500 oscillations, during which it underwent collisions with argon at a pressure of 9×10^{-6} Torr. The ion gained an average translational energy of 9.6 eV and an E_{cm} of 0.9 eV.

Table 1. Peak Assignments for SORI CID Spectrum of the BL_2^- Mannitol Borate Complex (m/z 371.1) Shown in Figure 5

fragment (m/z)	assignment
171.05	$C_6O_6H_{12}^{11}BO - ^2H_2O$
181.07	$C_6O_6H_{14} - H$
188.06	$C_6O_6H_{12}^{10}BO - H_2O$
189.06	$C_6O_6H_{12}^{11}BO - H_2O$
191.07	$C_6O_6H_{12}^{11}B$
206.07	$C_6O_6H_{12}^{10}BO$
207.07	$C_6O_6H_{12}^{11}BO$
352.13	$(C_6O_6H_{12})_2^{10}B - H_2O$
353.13	$(C_6O_6H_{12})_2^{11}B - H_2O$

Figure 5 shows a typical SORI CID spectrum. Table 1 shows the peak assignments. The peaks at m/z 353.1 and 352.1 are due to the loss of water from the ^{11}B and ^{10}B parent ions, respectively. As noted above, even though SORI CID was carried out on the ^{11}B parent only, some off-resonance excitation of the ^{10}B parent will also occur. It is interesting to note that the loss of water is a dominant fragmentation pathway in nearly all the ions observed. We have assigned the fragments at m/z 207.1 and 206.1 to the structure mannitol-B-O $^-$. Rose et al.⁷ observed a similar fragment when they used an increased cone voltage to induce fragmentation of a spiroborate. The presence of m/z 207.1 and 206.1 fragments confirms that the complex is composed of two sugar alcohols and a borate center, since these fragments are due to the loss of one sugar from BL_2^- . The fragments at m/z 188.1 and 189.1 result from the loss of water from m/z 206.1 and 207.1, respectively. The fragment at m/z 171.1 is due to the loss of two water molecules from m/z 207.1, although no ^{10}B analog is observed. We also observe a negatively charged ligand (mannitol) at m/z 181.1. The fragment at m/z 191.1 is postulated to be the loss of oxygen from m/z 207.1.

Borate Complexes of Carbohydrates Larger than Monosaccharides. Although we did not observe large oligosaccharides in the plant extracts studied here, Kobayaksi et al.¹⁴ did observe a complex of two 5 kDa sugars in radish root cell. Therefore, a number of larger sugars were investigated to determine whether the MALDI/FTMS method could be used to analyze borate complexes of larger sugars.

A sample containing 10 mM boric acid and 10 mM maltotriose was analyzed by MALDI/FTMS. Maltotriose is a trisaccharide

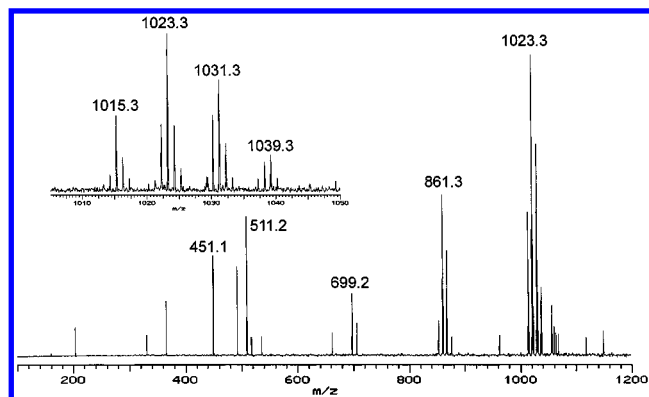


Figure 6. Negative mode MALDI/FTMS spectrum of 10 mM maltotriose with 10 mM boric acid sample. For other experimental details, see text.

of α -D-glucose and has 11 possible hydroxyl groups available to complex with the borate anion, compared with six in mannitol. Figure 6 shows the mass spectrum. The dominant peaks are found in the region from m/z 1010 to 1040, and the inset shows an enlarged view of this area. All the ions in this area are made up of two maltotriose units. The m/z 1015.3 peak corresponds to BL_2^- (where L is the doubly deprotonated maltotriose), the same stoichiometry as was seen in the mannitol and sorbitol spectra in the previous sections. The dominant ion is at m/z 1023.3, corresponding to a $B_2L_2H^-$ complex, with both borons as the ^{11}B isotopes, but now L corresponds to the quadruply deprotonated maltotriose [maltotriose - 4H] $^{4-}$. At m/z 1031.3, we observe a $B_3L_2H_2^-$ complex, with all three borons as the ^{11}B isotopes, and at m/z 1039.3, we observe a peak corresponding to $B_4L_2H_4^-$. Both of these species require more hydroxyl groups than are available to observe this many borate centers; i.e., we require 16 hydroxyl groups but only have available 11 in $B_4L_2H_3^-$. Therefore, at this high concentration of boron, we must be observing "polymers" of borate centers attached to the diols, i.e., R-O $_2$ -B-O $_2$ -B-(OH) $_2$. The isotopic distributions become increasingly complicated with the addition of boron to the complex.

Even at this high borate:sugar ratio (10:1), only a small amount of the trisaccharide-boron complex (BL^- , where L is quadruply deprotonated maltotriose) is observed, at m/z 511.2. In this case, the borate is attached to four hydroxyls on a single maltotriose. This is presumably because the maltotriose is flexible enough to bend into the correct conformation. Other peaks in the spectra include m/z 861.3, which reflects the loss of a glucose unit from m/z 1023.3, glycosidic bond cleavage being a common fragment in oligosaccharides, and m/z 699.2, corresponding to the loss of two glucose units from m/z 1023.3. We are unable to say whether these species were formed in the solution or are fragments from the MALDI process. The peak at m/z 451.1 is the loss of 60 u from m/z 511.2, an $^{0,2}A$ cross-ring cleavage,²³ another common oligosaccharide fragmentation pathway.

Maltoheptaose is an even larger oligosaccharide made up of seven glucose monomers, giving a possible 23 hydroxyl groups to complex with borate. The mass spectrum of 10 mM maltoheptaose and 10 mM boric acid is shown in Figure 7. The dominant ion is at m/z 1159.4, corresponding to a boron-maltoheptaose (BL^- , where L is [maltoheptaose - 4H] $^{4-}$) complex. No higher stoichiometries are observed in the mass spectrum.

(23) Domon, B.; Costello, C. E. *Glycoconjugate J.* **1988**, *5*, 397-409.

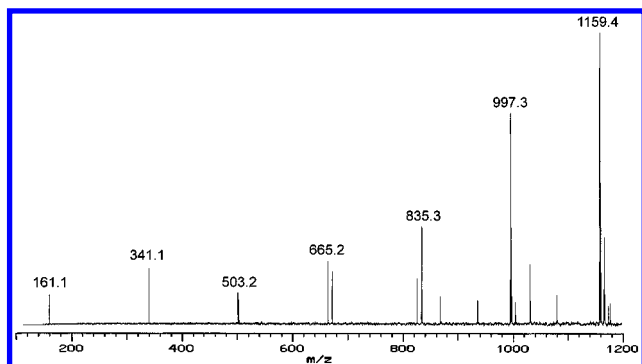


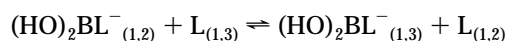
Figure 7. Negative mode MALDI/FTMS spectrum of 10 mM maltoheptaose with 10 mM boric acid solution. For other experimental details, see text.

The maltoheptaose chain is now flexible enough that it can orientate to complex a single borate anion, this being the exclusive complex seen. There are a series of sequential losses of glucose units at m/z 997.3, 835.4, 665.2, and 503.2. On-resonance CID of the m/z 1159.4 ion results in the formation of the m/z 997.3 ion (not shown). This is in contrast to the on-resonance CID of the mannitol borate complex, which was unsuccessful.

Further work is currently being carried out on other large oligosaccharides to see if borate complexation can be useful as an analytical tool to investigate structural features, such as branching,²⁴ of unknown sugars. The use of higher sugar:boric acid ratios should result in less complicated mass spectra compared to those shown in Figures 6 and 7.

Molecular Orbital Calculations of the Mannitol Borate BL_2^- Complex. During the MALDI/FTMS of the borate complexes, we believe we are truly observing complexes formed in the solution phase equilibrium. This is supported by the presence of the boron–DHB complex. It is unlikely that the borate complexes are being formed in the gas phase, since statistically it is unlikely that the three components would interact in the correct orientation during the short time the MALDI plume exists. Therefore, molecular orbital calculations on the sugar alcohol borate complexes possible in the solution phase equilibria (Scheme 1) may give insight into the possible gas phase structures.

Before semiempirical calculations were attempted on the borate complexes discussed above, calculations were performed on a previously studied system to check the validity of using the AM1 approach. Makkee et al.¹⁸ have calculated the stability constants of 1,2-propanediol and 1,3-propanediol borate esters in solution using ¹¹B NMR spectroscopy and obtained values of 1.4 and 0.9 l/mol, respectively. Using standard thermodynamic equations, these values gave $\Delta G = 0.26$ kcal/mol for the reaction,



where B is the borate anion and L is the [propanediol – 2H]²⁻ ligand. Using AM1, the predicted heats of formation were found to be –116.9 kcal/mol for 1,2-propanediol, –117.0 kcal/mol for 1,3-propanediol, –332.5 kcal/mol for $BL^-_{(1,2)}$, and –331.6 for $BL^-_{(1,3)}$. From these values, using standard thermodynamic equations, the ΔH of reaction is predicted to be 1.7 kcal/mol. We

Table 2. Heats of Formation (ΔH_f) of BL^- Complexes of Mannitol, Calculated Using AM1

“diol” carbons	ring size	ΔH_f (kcal/mol)
1,2	5	–550.10
2,3	5	–550.65
3,4	5	–551.19
1,3	6	–547.50
2,4	6	–547.94
2,5	7	–551.00
1,4	7	–549.58

can assume the entropic effects to be negligible between a five- and six-membered ring, and so the free energy of reaction is similarly 1.7 kcal/mol. The experimental value of 0.26 kcal/mol is in excellent agreement with the theoretical value, suggesting that AM1 provides reliable values for these systems. Previous work by Jacobson and Pizer²⁵ on trimethylboron anions also concluded that AM1 is a useful and accurate method for studying both structural and thermodynamic parameters of boron anions.

Although the BL^- species, where L is mannitol, was not observed in the MALDI/FTMS spectra, this system was studied using molecular orbital calculations as a model of the boron–sugar alcohol complex. Since the formation of the BL^- species is an integral step in the formation of the BL_2^- species (see Scheme 1), it is important to have a fully minimized structure of this intermediate; the heat of reaction (ΔH) for the BL^- species will have an effect on which BL_2^- coordinated species are formed. Mannitol was chosen since it has C_2 symmetry, making the possible number of combinations of borate esters less than that in the sorbitol system. Since there are a number of hydroxyls available for complexation in the mannitol ligand, we were interested to see which diol pairs were more favorable for complexation. The coordination, resulting ring size, and energy of the most stable structures are tabulated in Table 2. The results suggest that the six-membered rings are less energetically favorable than the five-membered rings. This may seem surprising, since we expect a six-membered ring to have less ring strain than a five-membered ring, as in the cyclic alkanes. However, upon examination of the bond lengths and bond angles, we see that the complexes differ from cyclic alkanes. In the $BL^-_{(1,3)}$ mannitol complex, the boron–oxygen bond lengths are 1.49 Å, shorter than a carbon–carbon bond length of 1.54 Å. In addition, the oxygen–boron–oxygen angle is 107°, more acute than the corresponding cyclohexane angle of 109°.

The apparent stability of the five-membered rings is also likely related to the relative orientation of the hydroxyl dipoles. For example, in the 3,4 complex, three of the hydroxyl groups appear to orientate toward the borate center. For the six-membered 1,3 complex, only two hydroxyl groups effectively interact with the borate. It is also possible that the mannitol is unable to adopt the lowest energy “zig-zag” conformation²⁶ when involved in a larger size ring. The seven-membered ring of the 2,5 complex may also seem like a surprisingly favorable orientation, but in this system there is once again a large interaction of the hydroxyl groups with the borate center.

Using the most favorable BL^- configurations, a number of BL_2^- systems were modeled since these species were observed in the

(25) Jacobson, S.; Pizer, R. *J. Am. Chem. Soc.* **1993**, *115*, 11216–11221.

(26) Kieboom, A. P. G.; Spoormaker, T.; Sinnema, A.; Toorn, J. M. v. d.; Bekkum, H. v. *Recl. Trav. Chim. Pays-Bas* **1975**, *94*, 53.

Table 3. Heats of Formation (ΔH_f) of BL_2^- Complexes of Mannitol, Calculated Using AM1

"diol" carbons	ΔH_f (kcal/mol)
1,2 1,2	-737.71
3,4 3,4	-741.93
1,2 3,4	-738.16
2,3 2,3	-737.09
3,4 2,3	-739.13
1,3 3,4	-738.09

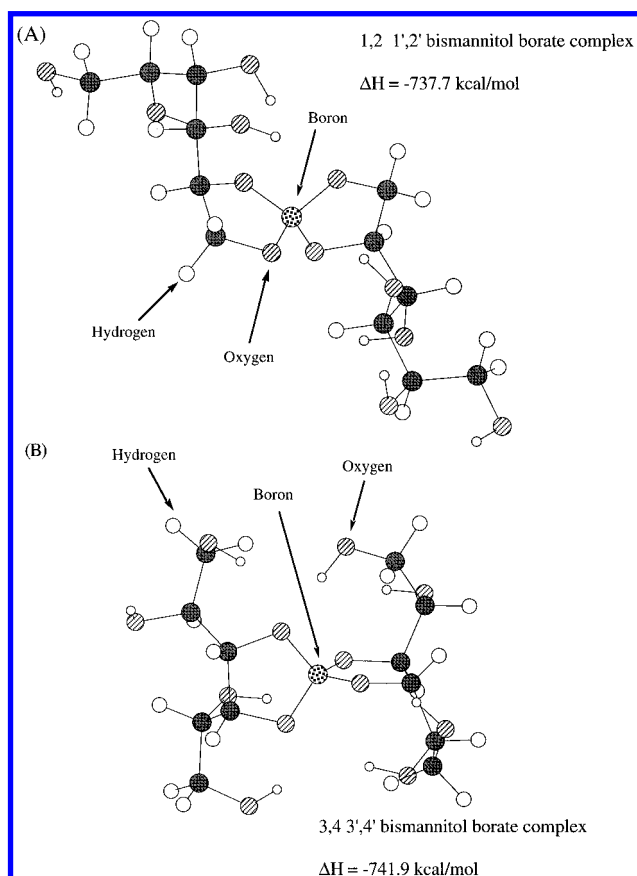


Figure 8. Optimized structures of anion (A) 1,2:1',2'-bismannitol borate and (B) 3,4:3',4'-bismannitol borate. Hydroxyl groups are orientated toward the borate atom.

mass spectra. Results for these molecular orbital calculations are shown in Table 3. Makkee et al.¹⁸ found from ¹¹B and ¹³C NMR that the 3- and 4-hydroxyl groups of mannitol bound preferentially with borate. This agrees well with the calculation results presented in Tables 2 and 3. From our molecular orbital calculations, the lowest energy conformer found for the 1,2:1',2' borate complex had $\Delta H_f = -737.7$ kcal/mol, whereas the 3,4:3',4' borate complex had $\Delta H_f = -741.9$ kcal/mol (Table 3). This result confirms the findings of Makkee et al.¹⁸ that the 3,4:3',4' borate ester is energetically more favorable by 4.2 kcal. Figure 8 shows the minimized structures of the 1,2:1',2' borate complex and the 3,4:3',4' borate complex. It is consistent that the heat of formation for the mixed diol complex of 1,2:3',4' borate ester has an intermediate value of -738.2 kcal/mol. There are a number of reasons for the greater stability of the 3,4 complexes. Makkee et al.¹⁸ postulate that borate ester formation involving the 1,2 positions is unfavorable because the terminal hydroxymethyl groups have a large freedom of rotation and, thus, complexation would result in an unfavorable change in entropy. Also, the 3,4

diols are in a preferential orientation, since mannitol adopts a zig-zag conformation in water.²⁶ However, based on the AM1 structures shown in Figure 8, it would appear that the 3,4:3',4' borate ester is favorable because the remaining uncomplexed hydroxyl groups form dipoles which point toward the borate center, hence solvating the charge center. In the 3,4:3',4' BL_2^- complex (Figure 8B), all the hydroxyl hydrogens are within 5 Å of the boron center (3.38, 2.72, 4.96, 3.72, 2.65, 3.75, 4.02, and 2.63 Å); however, in the 1,2:1',2' BL_2^- complex (Figure 8A), three of the hydroxyl protons are over 5 Å away, with the terminal hydroxyl group being 7.1 Å away (6.47, 3.53, 2.79, 2.66, 2.56, 3.92, 5.03, and 7.12 Å). All the BL_2^- complexes in Table 3 are made up of two five-membered rings, except the 1,3:3',4' complex. This is made up of a five-membered ring and a six-membered ring. The ΔH_f for this species appears to be an intermediate value (-738.09 kcal/mol).

CONCLUSIONS

In conclusion, we have clearly demonstrated that it is possible to observe sugar alcohol borate complexes using MALDI/FTMS. This work is important for understanding the mechanistic role of boron in plants. The results show that the complexes isolated from celery phloem sap, celery juice, and peach extracellular nectar are mainly composed of two mannitol or sorbitol molecules (L) complexed to a single borate center (B). In the case of peach extracellular nectar, the boron is also complexed to non-alditol monosaccharides, as well as alditols. Sustained off-resonance collision irradiation dissociation of the mannitol BL_2^- complex gives fragments that support the proposed structure. Complexes of larger oligosaccharides have also been successfully observed using MALDI/FTMS. Future work is planned on larger oligosaccharides to see if borate complexation can be useful as an analytical tool to investigate structural features, such as branching, of unknown sugars.

In addition, semiempirical calculations help toward a better structural understanding of the complexes by predicting the most favorable structure from the solution phase equilibrium. Semiempirical molecular orbital calculations (AM1) of the mannitol BL_2^- complex show that the most favorable configuration is that with carbons 3 and 4 of both mannitol residues complexed to the borate. This allows maximum interaction of the hydroxyl groups with the charged borate center.

ACKNOWLEDGMENT

C.B.L. and S.G.P. thank the National Institute of General Medical Sciences (NIH GM49077-01), the National Science Foundation (CHE-9531236), and the University of California for financial support. H.H. and P.H.B. are grateful to the U.S. Department of Agriculture (No. 9601359) and U.S. Borax for financial support. We also thank M. Kirk Green for generation of the predicted isotope pattern.

Received for review January 27, 1997. Accepted April 14, 1997.®

AC970101O

® Abstract published in *Advance ACS Abstracts*, June 1, 1997.